Collisional fragmentation of fast HeH^+ ions: The $He^{2+}+H^-$ channel

M. Barbatti,* L. P. G. de Assis, Ginette Jalbert, L. F. S. Coelho, I. Borges, Jr.,† and N. V. de Castro Faria
Instituto de Física, Universidade Federal do Rio de Janeiro, Caixa Postal 68528, Rio de Janeiro 21945-970, RJ, Brazil
(Received 22 April 1998; revised manuscript received 31 August 1998)

We studied the H^- production from the dissociation of fast HeH^+ projectiles, which occurs only through the $He^{2+}+H^-$ dissociative channel as electron capture is negligible at large velocities. We measured the lateral profiles of the H^- ions produced in collisions of HeH^+ with He and Ar atoms at velocities of 2.8, 4.0, and 4.9 a.u. and extracted from them an H^- kinetic energy distribution in the projectile center-of-mass frame. These results, together with a published internuclear distance distribution measured with a similar ion source, allowed us to obtain the potential energy curve associated to this dissociative channel. This energy curve crosses several excited states of the HeH^{2+} and HeH^+ ion dissociating into He^{2+} plus H and He^+ plus H, respectively, thereby suggesting the existence of an inhibition in the H^- formation process through transition to these HeH^{2+} and the HeH^+ states. The presence of this inhibition was corroborated by measuring the H^- total cross section for He, Ne, and Ar targets and $v=4$ a.u. [S1050-2947(99)01103-8]

PACS number(s): 34.90.+q

I. INTRODUCTION

Collisional excitation and destruction of simple molecules and small clusters are essential phenomena for a wide variety of research areas and, as such, have been the object of a rising interest in the last decades. For instance, low-energy collision processes, which are far from being understood, lead to the production of large organic molecules in the interstellar space and to the atmospheric concentrations of ozone and the greenhouse-effect gases (CO_2, NO_x, SO_x, etc.) in our planet. Molecular collision processes are also vital for producing atomic and molecular ions in cold plasmas, as the ones obtained in ion sources.

However important these processes are in nature, one must also remark that they present the common feature of being much harder to tackle than their atomic equivalents. Bound electronic states may possess hundreds of rovibrational levels, and cross sections are, for some processes, strongly dependent on these rovibrational levels. The interaction Hamiltonian for collision-induced molecular transitions is usually separated in nuclear and electronic terms, respectively, leading to rovibrational and electronic processes, in a Born-Oppenheimer framework and with the same limitations. There is also the intrinsic difficulty of obtaining the potential energy surfaces of the molecule and, in slow collisions, for the quasimolecule. All these complexities, mostly without correspondence in the atomic case, lead to very few calculations being available, even for the total destruction cross section of the simplest molecules, with a very limited range of energies and choice of projectiles and targets being found in the literature. The experimental situation is somewhat more comfortable than its theoretical counterpart but, the initial, the (eventual) intermediate, and the final states of the molecular projectile are usually incompletely known, as also is the final state of the target, and most of the experiments yield data integrated over several channels.

A very interesting collision process, not requiring detailed state-selection procedures, is the dissociation of fast two-electron molecular ions leading to the production of the negative ion H^-, as it follows a well-defined collision channel, if one is not concerned with the target final state. Firstly, as fast molecules are unlikely to capture electrons from the target and the final hydrogen nucleus carries the two electrons, the remaining nuclei (or nucleus) will be fully ionized. Secondly, the weakly bound hydrogen negative ion possesses only one bound state. Finally, if the projectile has electric dipole moment and travels a few microseconds from the ion source to the collision region, it is expected to be in the ground vibrational state and to present a Maxwell-Boltzmann rotational distribution, as experimentally verified by Kanter *et al.* [1] for HeH^+ ions produced in a rf ion source.

The most studied two-electron case is the production of H^- ions through the collisional dissociation of H_3^+ molecules. It has been investigated in detail by several authors [2] in the low velocity regime ($\sim 0.2 v_0$) and is usually interpreted as the three particle breakup $H_3^+ \rightarrow H^+ + H^+ + H^-$, electron capture being neglected. Experimental work has concentrated on determining, from the laboratory energy distribution of the scattered fragments, the total energy transferred to the H_3^+ ion, namely, Q, the kinetic energy W released during the collision, and the asymptotic angle between the two H^+ momenta in the projectile center-of-mass frame.

The $H_3^+ \rightarrow H^+ + H^+ + H^-$ case at high velocities, say, a few atomic units, has been studied by our group employing a method for determining the momenta of the outgoing fragments [3], available for fast particles. In short, the method uses the fact that the trajectories of the outgoing fragments of a high velocity molecular ion are confined to the interior of a narrow forward-directed cone, their angular deflections being a direct measure of the transverse velocity, provided the original parent beam is well collimated. The fragmentation process was assumed to be isotropic, i.e., there are no preferential directions of emission in the center-of-mass (c.m.)

*Electronic address: barbatti@if.ufrj.br
†Present address: Instituto de Química, Universidade Federal Fluminense, Morro do Valonguinho, 24020-150 Niterói, Brazil.

frame. Although anisotropies were reported as being important for transfer ionization and transfer excitation at larger relative velocities [4], where they are proposed to originate from interference of scattering amplitudes from the two atomic centers of the hydrogen molecule, in our velocity range, they are expected to be negligible. Under the assumption of the spectator model, the projectile nuclei do not change their momenta during the collision and, consequently, the transverse velocity of each fragment is equal to its c.m. velocity projected on the plane perpendicular to its trajectory. By employing a magnetic analyzer to separate the components under study from the original beam, the transverse velocity of the fragments can be determined by scanning the fragment beam profile at a sufficiently large distance downstream the collision site, leading to the c.m. energy distribution. The integral equation relating the measured lateral distribution to the c.m. one was numerically solved in reference [3], this computing procedure being improved in the present paper.

The presently studied $HeH^+ \rightarrow He^{2+} + H^-$ fragmentation channel is even simpler to measure and analyze. It does not require the positive ions to be detected in coincidence with the negative ones as they form asymptotically a two-particle system where, in the spectator model, the nuclei c.m. velocity in the laboratory frame remains unchanged. The HeH^+ fragmentation data, besides yielding the c.m. energy distributions for the H^- and the He^{2+} fragments, should depend only on the initial internuclear distribution, i.e., the square of the initial vibrational state wave function, and the potential energy curve of the corresponding excited molecular state, if one assumes the applicability of the reflection, or mirror, approximation [5]. The choice of projectile velocities larger than the orbital velocities of the target valence electrons led to a dissociation profile that was, essentially, target and velocity-independent. This profile together with a published HeH^+ internuclear distance distribution, measured by Kanter *et al.* [1] with a similar ion source, can allow an estimate for the potential energy curve associated to this dissociative channel.

According to the potential energy curves calculated by Michels [6], the HeH^+ ion preferentially breaks up as $He+H^+$. Another two-electron molecular projectile, the $H_3{}^+$ ion, also presents a H^- production cross section three orders of magnitude smaller than the one for its destruction, and this points to the presence of similar phenomena in HeH^+. As in the HeH^+ case, if one considered the excitation energies of the several channels of $H_3{}^+$ and employed simple statistical models for redistributing the electrons among the nuclei, a factor of only one order of magnitude would be expected. The lack of calculated $H_3{}^+$ potential energy surfaces did not allow a full understanding of which excited electronic states were responsible for the H^- inhibition; a discussion presented in Ref. [7] suggested states with C_{2v} nuclear geometries. The H^- production from the HeH^+ ion, with a simpler geometry, promised to be easier to understand.

II. EXPERIMENTAL ARRANGEMENT AND METHODS

A. Experimental setup

The experimental setup was described elsewhere [3]. In brief, the HeH^+ ion beam was obtained from the PUC-Rio 4 MV Van de Graaff accelerator employing its standard radio frequency ion source. The beam, after collimation to a diameter of less than 0.1 mm by a set of staggered crossed pairs of micrometric sliding slits, passed through a windowless differentially pumped gas target 10 cm long. The ratio of the pressures inside and outside the gas cell was approximately equal to 10^3.

Behind the gas target the incident beam and the reaction products passed through a magnetic analyzer, which separated the several charge-mass states. A silicon surface barrier detector was mounted at the 15° exit of the analyzing magnet in order to record the arrival of H^- ions coming from the dissociation of the incident HeH^+ ions and to determine their transverse spatial distributions. The distance between this detector and the gas target was 150 cm. It was verified that the original beam had a diameter still smaller than 0.15 mm at the position of the detectors. Distortions due to magnetic-field edge effects were observed to be negligible.

The transverse spatial distribution (''profile'') of the H^- fragment beam was determined first. Since, in the high velocity regime these ions are only produced through the $HeH^+ \rightarrow He^{2+} + H^-$ reaction channel, no coincidence was necessary but, even so, the incident beam current must be monitored for normalization purposes. This was done using a silicon surface barrier detector placed at $-15°$ that records the H^+ ions. The H^- ions were detected by a small silicon surface barrier detector fitted with a circular aperture of 0.35 mm diameter. The H^- beam was scanned by moving the detector along a line perpendicular to the magnet's plane of deflection across the exit opening. Care was taken to assure that the scanning line passed through the center of the fragment beam distribution. The recorded number of ions at each detector position was normalized to equal amounts of incident HeH^+ using the proton count.

The same basic setup was employed for the measurement of the H^- production cross section, the small surface barrier detector being replaced by a large one to avoid particle losses. The target pressure was measured by a thermocouple gauge, calibrated against a McLeod for each gas. The gas target thickness uncertainty was estimated as 10%, being due to the calibration procedure and the McLeod gauge uncertainty itself.

B. Center-of-mass energy distributions

A typical experimental transverse spatial distribution of the H^- ions is shown in Fig. 1. The observed shapes of the fragment beam distributions are entirely due to the asymptotic velocities of these fragments as the HeH^+ parent beam has a diameter experimentally verified to be smaller than 0.15 mm at the detector site and the target pressures corresponded to the single collision regime. It is then possible to extract the c.m. velocity distributions of the fragments from the shapes of their respective beam profiles, provided the spectator model is valid: Only the incident molecule electrons participate in the collision. This is reasonable since the projectile nuclei would only suffer an appreciable deflection when coming close to the nucleus of the target atom and the probability for this to happen is much smaller than the probability of electron-electron scattering. It is, therefore, assumed that the two nuclei are not disturbed

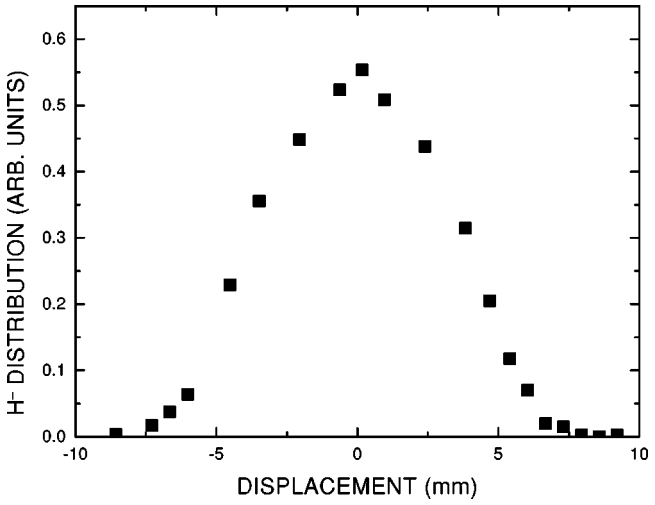

FIG. 1. A typical transverse spatial distribution of the H^- ions. The projectile velocity was 4.9 a.u. and the target was argon.

by the collision (except for a small loss in kinetic energy due to the excitation of HeH^+), implying that the total momentum of the molecular ion fragments is still equal to the projectile's initial momentum. On the other hand, the electronic configuration may be altered during collision and this, in the present case, leads to a self-dissociative excited state and subsequent molecule fragmentation.

An important assumption entering the data analysis is that the dissociation process occurs only within the gas target, i.e., no long-lived metastable intermediate state is formed. If such a state existed, dissociation could occur at a point closer to the detectors, and consequently, the fragments lateral dispersion at the detection plane would be smaller. This possibility, leading to a non-Gaussian shape for the lateral distribution, was not verified in the present experiments.

Qualitatively, it is clear that the width of a fragment's beam profile will increase with its c.m. velocity, $v_{c.m.}$, and that the observed shape of the beam profile will be the result of the contribution of many different velocities with appropriate weights. The transverse spatial distribution of fragments, $g(b)$, is given by the integral relation,

$$g(b)=\int_0^{\theta_m^M} N(b,\theta_m) f(\theta_m)\, d\theta_m, \tag{1}$$

where θ_m is the maximum deflection angle for a given $v_{c.m.}$, $N(b,\theta_m)$ is the transverse distribution for a given θ_m, $f(\theta_m)$ is the probability density function for this angle, and θ_m^M is the largest deflection angle for a given projectile energy.

The transverse spatial distribution of a fragment, $g_{fit}(b)$, was numerically generated from Eq. (1) and was compared to the smoothed experimental data, $g_{exp}(b)$. Briefly, this was done using the fact that $v_{c.m.}$ is related to the maximum deflection angle in the laboratory, θ_m, through the relation $\theta_m=\arctan(v_{c.m.}/v)$, where v is the initial projectile velocity. Assuming an isotropic orientation of $v_{c.m.}$ and taking into account the limited area of the detector, we have calculated $N(b,\theta_m)$ for a well defined value of $v_{c.m.}$ [3]. The next step was to choose a functional relation to c.m. velocity distribution of the H^- fragments. The best results were obtained for a Maxwell-Boltzmann type curve given by

$$f(\theta_m)=a_0[\theta_m+a_1(\theta_m)^2]\exp[-a_2(\theta_m-a_3)^2]. \tag{2}$$

The process was improved by a numerical fit of this analytical expression. Through its $\{a_i\}$ parameters, this distribution was changed in a systematic way, the integral in Eq. (1) was calculated and the result, $g_{fit}(b)$, compared to $g_{exp}(b)$ until a good fit had been obtained.

The c.m. energy distribution

$$f(E)=\frac{f(\theta_m)}{2A\beta\sec^2(\theta_m)\tan(\theta_m)}$$

$$=\frac{f(\theta_m)}{2A[E(\theta_m)+\beta][E(\theta_m)/\beta]^{1/2}}, \tag{3}$$

where $\beta=10^6E_0(\mathrm{MeV})/5$, A is the normalization constant, and $E(\theta_m)=\beta\tan^2(\theta_m)$, was considered satisfactory when the difference between the areas under the curves $g_{fit}(b)$ and $g_{exp}(b)$ was smaller than 3%.

C. H^- production cross sections

For low pressures and fast projectiles, no higher-order processes are present, such as H production followed by electron attachment in a subsequent collision, and the H^- fraction is a single collision process. Henceforth, this H^- yield is a linear function of the pressure, $F^-=\sigma^-x$, where σ^- is the H^- production cross section and x is the target thickness in atoms per unit area. Our cross section values were obtained in this region.

If one neglects electron capture, which leads to a small asymptotic value for the yield as the target thickness increases, the analytical expression for the yield is

$$F^-=\sigma^-\frac{\exp(-\sigma_d x)-\exp(-\sigma_l x)}{\sigma_l-\sigma_d}, \tag{4}$$

where σ_d is the destruction cross section of the HeH^+ [8] and σ_l is the electron loss cross section of H^- [9]. Cross section values were also extracted from the high-pressure region of this curve, if available, and compared with the ones coming from the growth rate method at low pressures, agreeing within 15%. In these cases an average was taken of both values and the error bar was estimated as 15%.

III. RESULTS AND DISCUSSION

The c.m. energy distributions of the H^- ions, all normalized to unity area, are displayed in Fig. 2, with their parameters being given in Table I. Assuming that no linear momentum is transferred between target and projectile, i.e., the so-called spectator model, the absolute values of the hydrogen and the helium linear momenta in the c.m. frame will be equal. The four c.m. energy distributions are similar to each other, as expected from the reflection (mirror) approximation [5], where the HeH^+ internuclear distance distribution is reflected to a dissociative state going into He^+ and H^-. This process is then interpreted as a noble gas valence electron

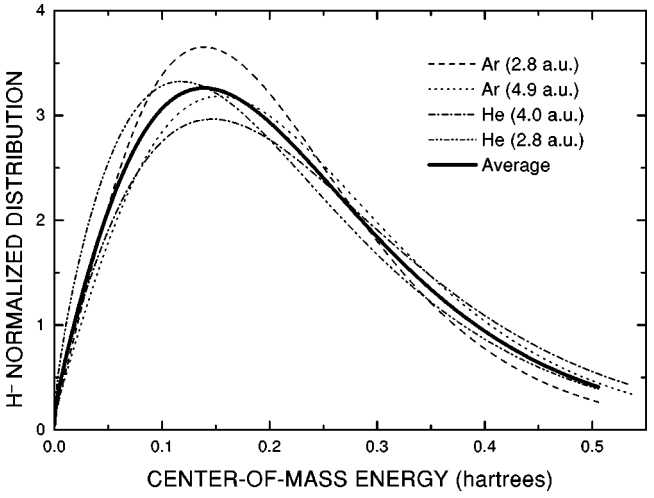

FIG. 2. The normalized center-of-mass energy distribution of the H^- ions. It was obtained by averaging distributions, also shown, coming from four different experiments.

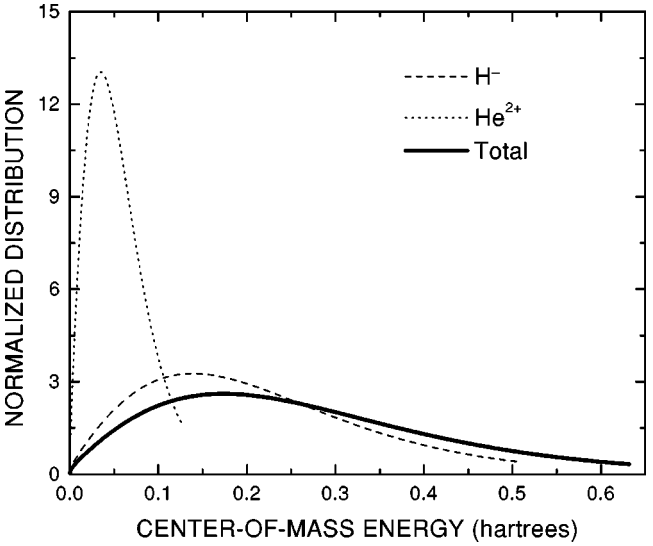

FIG. 3. H^-,He^{2+}, and total center-of-mass energy distributions, normalized to unity area.

colliding with the HeH^+ molecule and inducing a transition to an excited state. The He^{2+} and the total c.m. kinetic energies of the fragments are obtained by multiplying the H^- energy by 1/4 and 5/4, respectively, with the distributions, also normalized to unity area, being shown in Fig. 3.

As far as the authors are aware, there are no published values for HeH^+ potential energy curve of the presently studied dissociative state. Using the mirror approximation, it was possible to obtain this curve employing the total c.m. kinetic distribution (Fig. 3) and the internuclear distance distribution obtained by Kanter *et al.* [1] (Fig. 4). This potential energy curve was, subsequently, equalized, at a large internuclear distance, with the potential energy given by

$$E_p(R)=E_p^{\infty}-\frac{2}{R}-\frac{\alpha}{R^4},$$

with E_p^{∞} being the asymptotic energy and α the H^- polarizibility. The asymptotic energies for the ground and the presently studied states of the HeH^+ are, respectively, -2.9787 [10] and -0.5267 hartrees [11] and the H^- polarizibility is equal to 200 a.u. [12].

As already stated, there are no published values for HeH^+ potential energy curves for highly excited states such as the one studied in the present paper, although the understanding of this process would be greatly enhanced by this analysis as these states can either be intermediate steps for the presently studied state or be responsible for its destruction. There are, however, a few HeH^{2+} excited states (this ion is important as a three-body system with a well-known interaction) with asymptotic energies lying in this region, as calculated by Bates and Carson [13] (see Fig. 4), with more recent works being given in Ref. [14]. We can also estimate which HeH^+ levels, asymptotically leading to $He^+(n')+H(n)$, fall at the region of interest. As these two are hydrogenic systems, one has

$$E_{\infty}=-\left(\frac{4}{(n')^2}+\frac{1}{(n)^2}\right)0.5,$$

corresponding to states either with $n=1$ and $n'\geqslant 3 (E\geqslant -0.72$ hartrees) or with $n'=2$ and $n\geqslant 2$ $(E\geqslant -0.63$ hartrees).

While fast H particles coming from the fragmentation of these HeH^{2+} states could make single capture from the target atoms, this event being very unlikely at the MeV energy range, these HeH^+ excited states may play a more relevant role as an intermediate step in the H^- production. These HeH^+ states may have the outgoing H atom capturing the He^+ electron in a half-collision at eV energies. As this indirect mechanism would lead to structures in the c.m. energy distribution, and these were not observed, one can conclude that transitions to the presently studied state through these nearby HeH^+ excited states were not important.

Although presenting an overall agreement, a few points should be made concerning the four curves in Fig. 3. Firstly, the three parameters (peak, mean, and full width at half maximum) increase with the projectile energy both for the helium and for the argon targets, with the exception of the mean for the argon target. These energy and target dependences may be due (a) to a breakup of the Franck-Condon principle and the reflection rule, resulting in an energy-dependent transition element, (b) to target electron orbital velocities being comparable to the projectile velocity, henceforth going outside a free collision model framework, or (c) to an alignment effect between the molecular initial orienta-

TABLE I. H^- center-of-mass energies for He targets at (a) 2.8 a.u. and (b) 4.0 a.u.; for Ar targets at (c) 2.8 a.u. and (d) 4.9 a.u.: peak, mean, and FWHM values.

	H^- c.m. energy (hartree)		
Experiment	Peak	Mean	FWHM
(a)	0.118 ± 0.007	0.21 ± 0.01	0.273 ± 0.006
(b)	0.147 ± 0.008	0.24 ± 0.01	0.306 ± 0.006
(c)	0.140 ± 0.008	0.24 ± 0.01	0.254 ± 0.006
(d)	0.156 ± 0.009	0.23 ± 0.01	0.289 ± 0.006
Average	0.139 ± 0.009	0.23 ± 0.01	0.287 ± 0.006

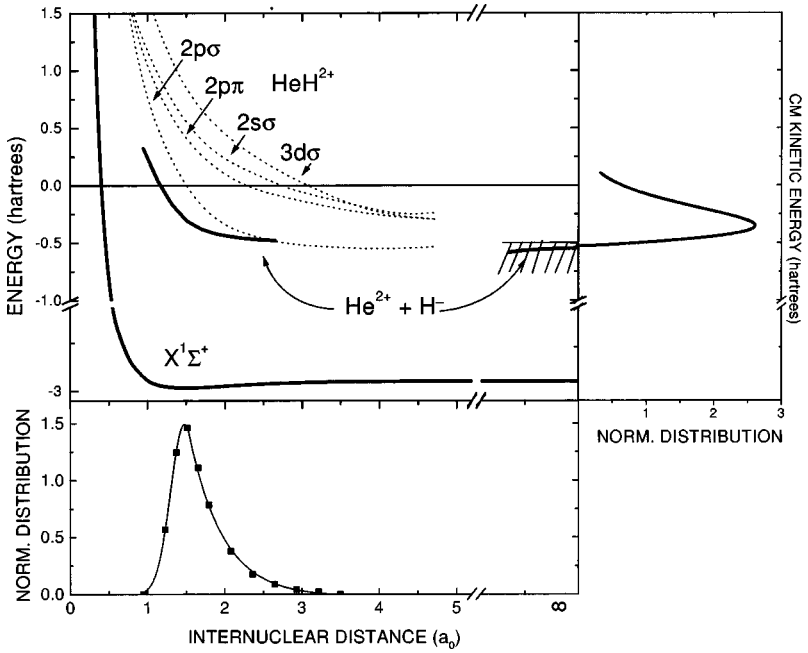

FIG. 4. Relevant electronic energies curves to H^- production from HeH^+. The electronic ground state is the $X^1\Sigma^+$, from Ref. [6]. The dissociative level was obtained from the experimental data, the internuclear distance distribution (bottom) taken from Ref. [1], and the normalized total c.m. energy distribution (right) as explained on the text. The curve of the total kinetic distribution was dislocated by a factor of -0.5267 hartrees, as it represents the distribution of kinetic energy above the dissociation limit. Excited states of HeH^{2+} are also shown. The hachured region represents the asymptotic energies of highly excited HeH^+ ions that break up as $He^+(n')+H(n)$.

tion and the beam direction. Concerning the first point, the Franck-Condon principle is just an approximation, and disagreements between its predictions and experimental results are well known in the literature [15]. The present case may be described, in a free collision model picture, as an almost free noble gas valence electron colliding with the HeH^+ molecule. As the projectile velocity is not so much larger than the orbital velocities of these electrons, the energy of this ''quasi-free electron'' in the projectile frame and, consequently, the transition elements may also be target-dependent. Finally, energy dependence may also arise from alignment effects [4] but, although in transfer ionization processes at high velocities they are present and increase with energy, no such effects were verified for double ionization and ionization excitation processes, even at large velocities. In short, small discrepancies appear among the four curves in Fig. 3 with several possible physical causes, and measurements in a wider energy range may be needed in order to clarify this situation.

Roughly, a very simple statistical model for the H^- production from HeH^+ fragmentation would be as follows: It will lead to an H^- ion if, at the instant of the collision, the two electrons are near the projectile proton. The probability for an electron to be near one nucleus is further assumed to be independent on the presence of another electron. With these very rough assumptions, in HeH^+ the probability for a departing nucleus to carry two electrons will be equal to 1/4. Nevertheless, the present experiment has yielded H^- production cross sections in He, Ne, and Ar targets at $v=4.0$ a.u., shown in Table II, which were three orders of magnitude smaller than the total HeH^+ destruction cross sections. Although expected in the grounds of comparison with a similar two-electron molecule, H_3^+, this result would indicate an inhibition process, where H^- is destroyed after being produced.

The potential energy curve for the $He^{2+}+H^-$ channel, estimated with the present results for the H^- c.m. distribution, lies very near to several HeH^{2+} curves dissociating either into He^+ and H^+ or into He^{2+} and H, and to HeH^+ curves dissociating into He^+ and H. This suggests that transitions to these states are the most likely source of inhibition of the H^- production. In particular, for the available c.m. energies, of the order a few eV, and the collision process $He^{2+}+H^-\rightarrow He^++H$, Peart and Bennet [16] got cross sections as high as 7×10^{-14} cm^2. This larger inhibition would then be probably associated to the transitions to HeH^+ states dissociating into $He^+(n')$ and H(1), due to the very small energy defects for these processes, the dominant states being those with n' equal to 3, 4, and mainly, 5. On the other hand, the potential curve for the H^- -producing dissociative state crosses several HeH^{2+} curves dissociating either into He^+ and H^+ or into He^{2+} and H. These states, $2p\sigma$, $2p\pi$, $2s\sigma$, and $3d\sigma$, are shown in Fig. 4, as calculated by Bates and Carson [13]. They may also play a role in the H^- inhibition, the transition presenting the smallest energy defect being associated to the single ionization of H^- perturbated by the He^{2+} field, and producing $He^{2+}+H(1s)+e^-$.

IV. CONCLUSIONS

The center-of-mass energy distribution has been obtained for H^- originating from the collisional dissociation process $HeH^+\rightarrow He^{2+}+H^-$ at high projectile velocities, from four different sets of data. The four c.m. energy distributions present an overall similarity, showing the overall validity of the simple reflection picture and of this averaging procedure. There are, however, small energy and target dependences,

TABLE II. H^- production cross sections, $\sigma(HeH^+\rightarrow H^-)$, at $v=4.0$ a.u. in He, Ne, and Ar targets (10^{-19} cm^2).

Target element	$\sigma(HeH^+\rightarrow H^-)$ (10^{-19} cm^2)
He	0.24 ± 0.03
Ne	0.99 ± 0.15
Ar	1.40 ± 0.21

suggesting the need for further measurements in a wider energy range and with heavier targets.

The total c.m. energy distribution, together with a published internuclear distance distribution measured with a similar ion source, allowed obtaining the potential energy curve associated to this dissociative channel. The knowledge of this curve, neither calculated nor measured before, is relevant for understanding the H^- production results, also measured in the present paper.

Considering the H^- production cross sections, measured for He, Ne, and Ar targets at $v=4$ a.u., the H^- yields (σ^-/σ_d) for these three targets agree within 20%, thereby showing that possible target dependences are smaller than this percentual value. The indirect mechanism of H^- production, fragmentation into H and He^+ followed by electronic capture from He^+, is not important as was indicated by the lack of structures in the c.m. total kinetic energy distribution.

The smallness of the H^- yields, of the order of 10^{-3}, points to an inhibition in the process of H^- formation, with one H^- electron being, in a second step, transferred to the He^{2+} ion or even to the continuum. Analyzing the electronic states of the HeH^+ molecule, one notices that the potential energy curve for the present channel lies very near to several HeH^{2+} curves and also that, asymptotically, it comes very near to several HeH^+ states dissociating into He^+ and H. It is thereby suggested that transition to these HeH^+ and HeH^{2+} states may lead to the inhibition process, the relative importance of each channel requiring further theoretical work.

ACKNOWLEDGMENTS

This work was partially supported by CNPq and FINEP. We acknowledge the assistance from the technical staff of the PUC-Rio Van de Graaff Laboratory.

[1] E.P. Kanter, P.J. Cooney, D.S. Gemmell, K.-O. Groeneveld, W.J. Pietsch, A.J. Ratkowski, Z. Vager, and B.J. Zabransky, Phys. Rev. A **20**, 834 (1979).

[2] D.L. Montgomery and D.H. Jaecks, Phys. Rev. Lett. **51**, 1862 (1983); D.H. Jaecks, O. Yenen, C. Engelhardt, and L. Wiese, Nucl. Instrum. Methods Phys. Res. B **40/41**, 225 (1989); O. Yenen, D.H. Jaecks, and L.M. Wiese, Phys. Rev. A **39**, 1767 (1989); I. Alvarez, H. Martinez, C. Cisneros, A. Morales, and J. de Urquijo, Nucl. Instrum. Methods Phys. Res. B **40/41**, 245 (1989); I. Alvarez, C. Cisneros, J. de Urquaijo, and T.J. Morgan, Phys. Rev. Lett. **53**, 740 (1984).

[3] N.V. de Castro Faria, W. Wolff, L.F.S. Coelho, and H.E. Wolf, Phys. Rev. A **45**, 2957 (1992).

[4] S. Cheng, C.L. Cocke, V. Frohne, E.Y. Kamber, J.H. McGuire, and Y. Wang, Phys. Rev. A **47**, 3923 (1993).

[5] G. Herzberg, *Spectra of Diatomic Molecules* (Krieger Publishing Company, Malabor, FL, 1984), Vol. I.

[6] H.H. Michels, J. Chem. Phys. **44**, 3834 (1966).

[7] K.C. Kulander and M.F. Guest, J. Phys. B **12**, L501 (1979).

[8] L.F.S. Coelho, Ginette Jalbert, I. Borges, Jr., and N.V. de Castro Faria, J. Phys. B **29**, 733 (1996).

[9] D.P. Almeida, N.V. de Castro Faria, F.L. Freire, Jr., E.C. Montenegro, and A.G. de Pinho, Phys. Rev. A **36**, 16 (1987).

[10] W. Cencek, J. Komasa, and J. Rychlemski, Chem. Phys. Lett. **246**, 417 (1995).

[11] M.T. Fontenelle, M.R. Gallas, and J.A.C. Gallas, J. Phys. B **19**, L639 (1986).

[12] M. Terao, C. Harel, A. Salin, and R.J. Allan, Z. Phys. D **7**, 319 (1988).

[13] D.R. Bates and T.R. Carson, Proc. R. Soc. London, Ser. A **234**, 207 (1956).

[14] I. Ben-Itzhak, I. Gertner, O. Heber, and B. Rosner, Phys. Rev. Lett. **71**, 1347 (1993).

[15] F. von Busch and G.H. Dunn, Phys. Rev. A **5**, 1726 (1972).

[16] B. Peart and M.A. Bennet, J. Phys. B **19**, L321 (1986).